

Design and characterization of a tunable polarization-independent resonant grating filter

Guido Niederer, Wataru Nakagawa and Hans Peter Herzig

Institute of Microtechnology, University of Neuchâtel, Rue A.-L. Breguet 2, 2000 Neuchâtel, Switzerland
hanspeter.herzig@unine.ch

Hans Thiele

Centre Suisse d'Electronique et de Microtechnique (CSEM), Badenerstrasse 569, 8048 Zürich, Switzerland

Abstract: We present the design, analysis and characterization of a polarization-independent tunable resonant grating filter. Polarization independence is achieved by setting the plane of incidence parallel to the grating grooves and optimizing the fill factor to obtain a strong reflection peak for all incident polarization states. Experimental measurements show that approximate angular insensitivity to the input polarization orientation concurrent with tunability over a wavelength range of roughly 1530 nm to 1560 nm is achieved. Modulation of the reflectivity peak shape with variations in the orientation of the incidence plane are observed, and found to be in qualitative agreement with theoretical predictions.

References and links

1. J. M. Bendickson, E. N. Glytsis, T. K. Gaylord, and D. L. Brundrett, "Guided-mode resonant subwavelength gratings: effect of finite beams and finite size," *J. Opt. Soc. Am. A* **18**, 1912-1928 (2001), and references therein.
2. G. Niederer, H. P. Herzig, J. Shamir, H. Thiele, M. Schmieper, Ch. Zschokke, "Tunable, oblique incidence resonant grating filter for telecommunications," *Appl. Opt.* **43**, 1683-1694 (2004).
3. D. Lacour, G. Granet, J.-P. Plumey and A. Mure-Ravaud, "Polarization independence of a one-dimensional grating in conical mounting," *J. Opt. Soc. Am. A* Vol. **20**, 1546-1552 (2003).
4. A. L. Fehrembach, A. Sentenac, "Study of waveguide grating eigenmodes for unpolarized filtering applications," *J. Opt. Soc. Am. A* **20**, 481-488 (2003).
5. A. Mizutani, H. Kikuta, K. Nakajima and K. Iwata, "Nonpolarizing guided-mode resonant grating filter for oblique incidence," *J. Opt. Soc. Am. A* **18**, 1261-1266 (2001).
6. G. Niederer and HP Herzig, "Modeling polarization independent resonant grating filters," Conference Digest, *Diffraction Optics 2003*, Oxford, UK.
7. M. G. Moharam, E. B. Grann, D. A. Pommet and T. K. Gaylord, "Formulation for stable and efficient implementation of the rigorous coupled-wave analysis of binary gratings," *J. Opt. Soc. Am. A* **12**, 1068-1086 (1995).
8. D. Lacour, PhD-thesis, "Diffraction d'une onde plane par un guide périodique: application à la conception d'un filtre en longueur d'onde indépendant de la polarisation," Université Blaise Pascal, Clermont Ferrand, France (2002).

1. Introduction

Resonant grating filters (RGFs) offer the possibility to create a narrow band reflection filter with a relatively simple fabrication process [1,2]. Fundamentally, the device consists of a waveguide plus a grating, such that at resonance the incident light is coupled via the grating into a waveguide mode. Most previous work has focused on the configuration where the plane

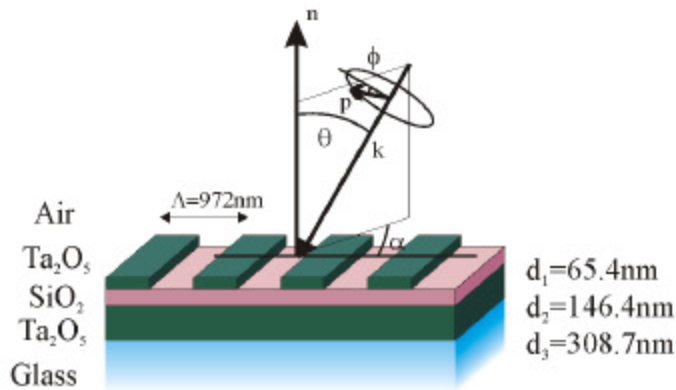


Fig. 1. Polarization independent RGF, working around $\theta=45^\circ$ angle of incidence (AOI) with a conical angle (α) of 90° . The grating fill factor is $F=0.475$. The refractive indices are $n_{\text{Ta}_2\text{O}_5}=2.066$, $n_{\text{SiO}_2}=1.444$, $n_{\text{Glass}}=1.51$, and $n_{\text{Air}}=1.0$.

of incidence is perpendicular to the grating grooves (the so-called classical mount corresponding to $\alpha=0^\circ$ in Fig. 1) [1], as the design and analysis of the grating performance is greatly simplified. However, for a single-mode waveguide, only a single polarization-independent solution exists [3], meaning a tunable polarization-independent device is not possible. Consequently, we consider the orthogonal incidence plane, parallel to the grating grooves. In this case, the two input polarization states *s* and *p* (E field normal to or in the incidence plane, respectively) both excite a pair of waveguide modes having mirror symmetry with respect to the incidence plane, fulfilling the conditions for efficient (theoretically up to 100%) polarization-independent filtering [4]. It should be mentioned that using a 2D grating, other solutions exist [5,6] but they do not offer additional advantages for our application and are more difficult to fabricate. A low-cost polarization-independent optical filter has a large number of applications, for example as an add/drop filter in a long-haul (fiber-based) communication system, where it is not easy to maintain a fixed polarization state.

2. Theory

In this paper we present the design and characterization of a polarization-independent RGF. Polarization independent operation is achieved by setting the plane of incidence parallel to the grating grooves. In this configuration, a linearly polarized input optical field can, in general, couple to both TE and TM polarized modes in the waveguide, but under different resonance conditions. This fact consequently implies that the two linear polarization components *s* and *p* of an arbitrary input polarization state can both couple into like (i.e. either TE or TM) modes in the waveguide, again generally under differing resonance conditions. In addition, if both polarization components couple into only TE or only TM modes, tunable operation may be achieved. By optimizing the grating parameters for a specific wavelength, incidence angle, and waveguide mode, the resonance conditions corresponding to the *s*- and *p*-components of the input field can be made to coincide, resulting in high reflectivity from the device at a certain wavelength regardless of the input polarization orientation.

The device is a three-layer stack consisting of a planar waveguide, a separation layer, and a rectangular grating on top with a grating period of 972 nm. The grating and the waveguide are made of Ta_2O_5 ($n=2.066$), the separation layer is SiO_2 ($n=1.444$) and the substrate is glass ($n=1.51$). The separation layer gives an additional degree of freedom to achieve antireflective conditions for the incident light, and also is useful as an etch-stop in the fabrication process. The thickness of the grating layer primarily affects the coupling strength between the input light and the waveguide modes, and is chosen to achieve the desired resonance line width. The thicknesses of the grating and separation layers also affect the off-resonance reflectivity of the device, and are optimized in order to minimize the accumulated reflectivity of incident *s*- and *p*-polarization and to show an average (*s*- and *p*-polarization) reflection resonance linewidth of 1nm at $\lambda=1545\text{nm}$ at 45° angle of incidence. The resulting element is shown in

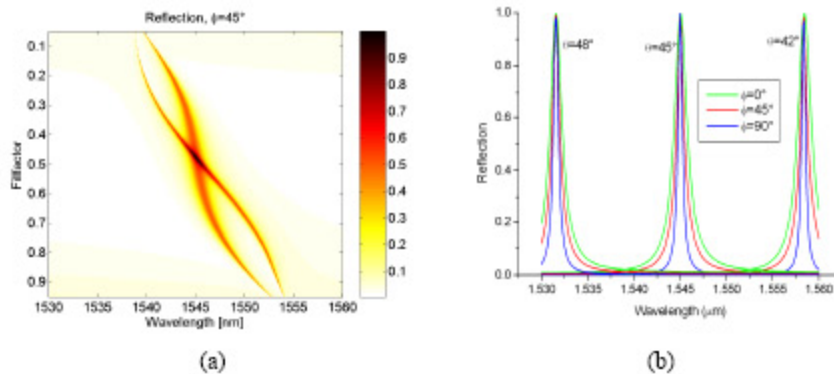


Fig. 2. Spectral reflectivity of the element shown in Fig. 1 for linearly polarized light. For (a) polarization angle $\phi=45^\circ$ and AOI $\theta=45^\circ$ with continuous variation of the fill factor and (b) three different AOIs θ , each with three different polarization angles ϕ , assuming a fill factor of $F=0.475$.

Fig. 1. Using rigorous coupled wave analysis [7], the reflectivity for an incident plane wave linearly polarized at $\phi=45^\circ$ as a function of the wavelength and the grating fill factor is computed and presented in Fig. 2(a). In most instances, two resonances are found, corresponding to the coupling of the s- and p-components of the input field into TE modes in the grating. The coupling between the two waveguide modes is weak enough that no peak splitting is visible. The reflectivity is maximal for $\lambda=1545\text{nm}$ and a grating fill factor of $F=0.475$. In principle, coupling into grating TM-modes is also possible, and yields two intersection points with fill factors of $F=0.25$ and $F=0.8$. However, since a fill factor near $F=0.5$ is easier to fabricate, we investigate the TE case.

The reflectivity as a function of wavelength for three different angles of incidence (AOI) and for three different polarization orientations is shown in Fig. 2(b). These results show that the position of the reflection peaks are independent of polarization. At 45° AOI, the spectral linewidth for the s-polarization ($\phi=90^\circ$) is 0.56nm and for the p-polarization ($\phi=0^\circ$) is 1.64nm , a factor of 2.92 different, because the coupling efficiency depends on the polarization state. The linewidth of all other polarization states lie between these two values. The variation in the spectral linewidth could be a problem in some applications; however in [8] it is shown that this effect can be reduced by changing the central incidence angle. For all AOI and polarization angles, the theoretical peak reflectivity, in the absence of absorption, reaches 100%. The fact that for a given AOI the reflection maximum occurs at the same wavelength for all polarization states offers the potential to use this device in a tunable configuration. The peak reflection wavelength is determined by selecting the AOI. When considering the tolerances, we notice a fundamental difference between the classical-mount polarization-dependent element and the polarization-independent element under study. In the classical mount, a deviation of 1° in the conical angle has only a small influence. A small deviation in the conical angle (e.g. due to assembly of the device) of the polarization-independent element immediately results in a spectral peak splitting with reduced efficiency. The dependence on the conical angle for incoming p-polarized light is illustrated in Fig. 3(a), assuming a grating fill factor of $F=0.5$. A deviation of 0.05° in the conical angle results in the reduction of the peak reflectivity from 100% to 87% and the appearance of a second peak. Consequently, a higher orientation and alignment accuracy is required in order to obtain good performance with the polarization-independent element.

3. Measurement

The element is fabricated by first depositing three thin film layers on a glass substrate. After the lithographic step the grating is transferred into the topmost layer, resulting in a rectangular grating shape [2]. AFM measurements reveal that the grating fill factor is slightly higher than the design value of $F=0.475$, and is approximately 0.50. The grating height is about 60nm . On

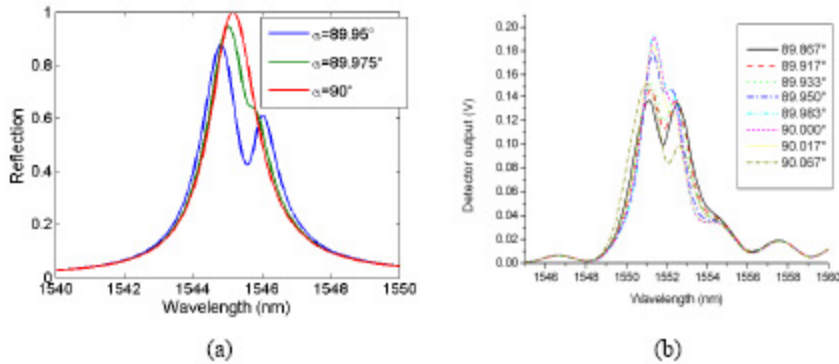


Fig. 3. Dependence of the reflection peak on the conical angle α . (a) Theoretical curve for the device of Fig. 1, but with a grating fill factor of $F=0.5$ for incident p-polarization ($\phi=0^\circ$); (b) Measured spectral reflectivity of the fabricated device. The measured resonance wavelength is shifted towards longer wavelengths.

the backside of the element a two layer AR-coating is deposited. The fabricated sample is placed on a rotation stage and is illuminated by a collimated linearly polarized beam. The reflection and transmission are measured simultaneously with two different detectors. First the spectral reflection as a function of a change in the conical angle for p-polarized incident light is measured and shown in Fig. 3(b). The measured peak splitting shows good agreement with the theoretical computations of Fig. 3(a). Due to the configuration of the measurement apparatus, there is an uncertainty in the origin of the conical angle (α) that is removed using the symmetry of the peak reflectivity around its maximum value corresponding to $\alpha=90^\circ$. The ripples on both sides of the peaks are due to Fabry-Perot interference caused by imperfect AR coatings. The measured resonance wavelength differs slightly from the design. By adjusting the AOI, it is possible to bring the resonance back to the desired wavelength. Finally, we measured the spectral response for three different AOI each with three different polarization states, as shown in Fig. 4. We show transmissivity as opposed to reflectivity because the error bounds for the correct normalization in reflection were too large. For each AOI the resonance peaks for all three input polarizations occur approximately at the same wavelength. As predicted by the theory, the reflectivity peak for the p-polarization is higher and wider than for the s-polarization. The width and efficiency for the 45° incident polarization is between

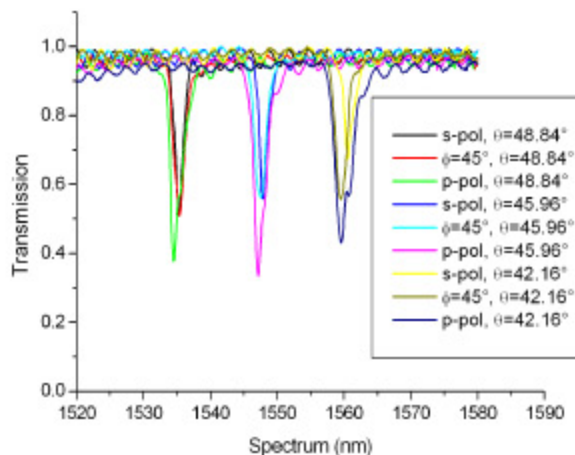


Fig. 4. Measured spectral transmission for three different AOIs θ and three different polarization orientations ϕ .

the values of the two fundamental polarizations. We can observe two main reasons for the differences between the measurement and theory. Firstly the illumination was not a plane wave (standard collimator with 1mm beam diameter and aberrations) resulting in an increased angular spectrum of the incident beam and thus a decreased efficiency and slightly wider peaks. Secondly, the rotation axis for the AOI was not perfectly aligned with respect to the incident beam and the sample. Consequently a change of the AOI also induces a small change in the conical angle. A misalignment of 1° between the rotation axes in combination with a change of 3° in the AOI induces a change of the conical angle between 0.001° and 0.05° , depending on the deviation of the rotation axis orientation. From theory we have seen that a change of 0.05° in the conical angle results in a severe drop in efficiency and a distortion of the peak shape.

4. Conclusion

We have designed and fabricated a polarization independent tunable RGF with a simple grating. Although more work is needed to better control the fabrication process and to reduce the misalignment, we demonstrate that it is possible to fabricate a polarization independent tunable RGF. The combination of relatively simple fabrication (only three thin film layers, and only one structured layer), the potential for polarization-independent operation, and the tunability of the filter makes this class of devices a good candidate for use with a fiber-based long haul communication system.

Acknowledgments

The authors acknowledge the financial support of the Centre Suisse d'Electronique et de Microtechnique (CSEM).